Extremal paths, the stochastic heat equation, and the three-dimensional Kardar-Parisi-Zhang universality class

Timothy Halpin-Healy
Physics Department, Barnard College, Columbia University, New York, New York 10027, USA
(Received 21 July 2013; revised manuscript received 11 September 2013; published 10 October 2013)

Following our numerical work [Phys. Rev. Lett. **109**, 170602 (2012)] focused upon the $2+1$ Kardar-Parisi-Zhang (KPZ) equation with flat initial condition, we return here to study, in depth, the three-dimensional (3D) radial KPZ problem, comparing common scaling phenomena exhibited by the pt-pt directed polymer in a random medium (DPRM), the stochastic heat equation (SHE) with multiplicative noise in three dimensions, and kinetic roughening phenomena associated with 3D Eden clusters. Examining variants of the 3D DPRM, as well as numerically integrating, via the Itô prescription, the constrained SHE for different values of the KPZ coupling, we provide strong evidence for universality within this 3D KPZ class, revealing shared values for the limit distribution skewness and kurtosis, along with universal first and second moments. Our numerical analysis of the 3D SHE, well flanked by the DPRM results, appears without precedent in the literature. We consider, too, the $2+1$ KPZ equation in the deeply evolved kinetically roughened *stationary state,* extracting the essential limit distribution characterizing fluctuations therein, revealing a higher-dimensional relative of the $1+1$ KPZ Baik-Rains distribution. Complementary, corroborative findings are provided via the Gaussian DPRM, as well as the restricted-solid-on-solid model of stochastic growth, stalwart members of the $2+1$ KPZ class. Next, contact is made with a recent nonperturbative, field-theoretic renormalization group calculation for the key universal amplitude ratio in this context. Finally, in the crossover from transient to stationary-state statistics, we observe a higher dimensional manifestation of the skewness minimum discovered by Takeuchi [Phys. Rev. Lett. **110**, 210604 (2013)] in $1+1$ KPZ class liquid-crystal experiments.

DOI: 10.1103/PhysRevE.88.042118 PACS number(s): 05.40.−a, 05.10.Gg

I. INTRODUCTION

Random walks are ubiquitous in nature, whether they be the financial meanderings of a trader on Wall Street, the thermal diffusions of heat in a solid, the fluctuations of vortex lines in a high-T_c superconductor, or the erratic trajectories of a firefly on a late summer's eve. The mathematical theory underlying the universality of such paths has at its center the Gaussian distribution, figuring prominently in the solution of diffusion, heat, and Schrödinger equations, cornerstones of theoretical physics. A complementary, but much more mathematically rich, modern, and technically challenging problem considers random walks in a landscape which is, itself, random. The focus then is on the statistical properties of the globally optimal path through this random landscape, a delicate dimension-dependent affair. In a two-dimensional (2D) random medium [1], the statistics of these directed extremal paths is known exactly due to impressive recent work [2] and is governed by a superuniversal *non*-Gaussian distribution of great mathematical import, originally discovered by Tracy and Widom [3] in the context of random matrix theory [4]. Via serendipitous mappings, this skewed, asymmetric probability distribution [5] connects a host of seemingly unrelated problems, including the nonequilibrium roughening of flameless fire lines [6], turbulent liquid crystals [7], stochastic growth models such as ballistic deposition and Eden [8], as well as the shock-laden kinetics of one-dimensional (1D) driven lattice gases [9], the last providing an intriguing toy model of motor protein traffic flow [10]. All, however, are manifestations of an extraordinary nonlinear stochastic PDE due to Kardar *et al.* [11], proposed more than a quarter century ago.

In this paper, we revisit [12] the three-dimensional (3D) case, where no exact results exist. Investigating a collection of systems selected from different vantage points, (a) 3D pt-pt extremal paths, (b) Itô integration of the 3D stochastic heat equation (SHE), and (c) surface roughening of 3D Eden clusters, we invoke scaling arguments to strip the results of model-dependent baggage, isolating the essential mathematical object, and extract the universal limit distribution at the heart of the 3D Kardar-Parisi-Zhang (KPZ) class. We start with the KPZ equation itself, which, in the growth model context, characterizes the fluctuations of the height $h(\mathbf{x},t)$ of a kinetically roughened interface:

$$\partial_t h = \nu\nabla^2 h + \tfrac{1}{2}\lambda(\nabla h)^2 + \sqrt{D}\eta,$$

where ν, λ, and D are phenomenological parameters, the last setting the strength of the stochastic noise η. A Hopf-Cole transformation, $h = \frac{2\nu}{\lambda}\ln Z$, maps KPZ dynamics onto the equilibrium statistical mechanics of directed polymers in random media; i.e., the stochastic heat equation with multiplicative disorder, governing the restricted partition function $Z(\mathbf{x},t)$ of the directed polymer in a random medium (DPRM):

$$\partial_t Z = \nu\nabla^2 Z + (\lambda\sqrt{D}/2\nu)Z\eta,$$

itself, via the extremal path interpretation, a classic model of ill-condensed matter physics but, mathematically, a deeply nuanced, intractable and unscalable Everest in its own right [13]. We begin our own ascent here (to an admittedly low-level base camp), numerically solving the 3D SHE in pt-pt, pt-line, and pt-plane geometries, illustrating its undeniable kinship to the KPZ equation.

II. 3D PT-PT KPZ CLASS

Formal solution of 3D SHE can be cast in the guise of a Feynman path integral, which, discretized on a lattice and evaluated at zero temperature, inspires transfer matrix studies

of DPRM extremal trajectories. Here we examine specifically the 3D *pt-pt* problem; the matter is seductively simple to pose: Consider a directed walk through a 3D cubic lattice, the ith site of which possesses a random energy ε_i drawn from uniform (u), Gaussian (g), or exponential (e) distributions. The trajectory proceeds from one crystallographic plane (i.e., "time slice") to the next, the total energy of a path of t steps being the sum $E(t) = \sum \varepsilon_i$ of the site energies collected along the way. Our walks are oriented, on average, along the [001] or [111] directions. In the latter instance, with trajectories cutting diagonally through the lattice, there are three available sites at each step, all geometrically equivalent; these extremal paths link far corners of a cube. In the former case, with walks aligned in an axial direction, there are five immediate neighbors in the next crystal plane, four involving a sidestep, which incur an energy cost γ, a *tunable* microscopic elasticity parameter. These extremal paths, by contrast, connect centers of opposing faces of the cube. Either way, however, these are pt-pt extremal paths that we are considering, with both the departure point and terminus of the trajectory fixed. Averaging over many realizations of disorder, we are concerned with the statistical fluctuations, $\delta E = E - \langle E \rangle$, about the mean for the extremal trajectory through this 3D random energy landscape. Here we consider (i) $u5_1$ DPRM: random site energies *uniformly* drawn from the interval [0,1]; travel direction = [001]; elastic energy cost, $\gamma = 1$, for transverse steps, (ii) $g5_1$ DPRM: *Gaussian* energies of zero mean, variance 1/4, transverse steps incur, again, unit cost; (iii) $g5_{1/2}$ DPRM, the same, but $\gamma = 1/2$; and finally, (iv) $e3$ DPRM: proceeds diagonally; unit mean, *exponentially* distributed random site energies, no elastic cost and paths connect far corners of the cube. These four DPRM workhorses form the foundation of our present analysis of the 3D KPZ class; three had been employed previously (not $g5_{1/2}$) in our earlier investigation of the $2+1$ *pt-plane* KPZ problem, which entailed seven models [12]. In fact, we include here additional $2+1$ Eden and SHE pt-plane results; see later, for that particular geometry, as well as a full consideration of the stationary-state statistics therein. The 3D pt-line KPZ class, a separate matter, is addressed in the Appendix.

A. Universality: first pass

In Fig. 1 we reveal the 3D pt-pt fluctuation PDFs associated with our four DPRM models, along with two distinct numerical integrations of the constrained $2+1$ SHE, allowing for different values of the KPZ parameter λ. Our study of the 3D SHE relies upon the Itô interpretation of an elemental, rescaled version of the stochastic partial differential equation:

$$\partial_t Z = \nabla^2 Z + \sqrt{\epsilon} Z \eta + \frac{\epsilon}{2} Z,$$

laid out, years ago, by Beccaria and Curci [14], who sought, back then, to extract $2+1$ KPZ exponents in a *pt-plane* setup. Here we study $\sqrt{\epsilon} = \lambda\sqrt{2D/\nu^3} = 6$ and 12, the latter placing us very deep, indeed, within the strong coupling KPZ regime. For all the DPRM simulations, and SHE integrations, we have evolved the system through the forward and rear light cones of the initial and final points of the trajectory, averaging over 10^7 runs, considering paths of $t = 500$ steps.

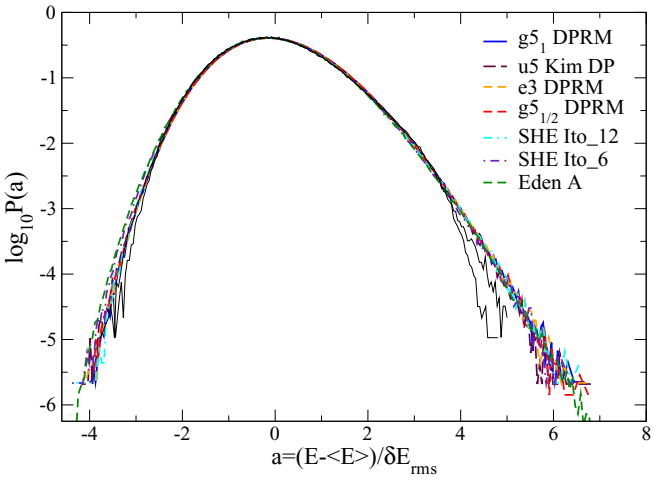

FIG. 1. (Color online) Fluctuation PDFs: 3D *radial* KPZ class.

The numerical demands of this enterprise are rather severe, however, and in sharp contrast to the pt-plane problem. For our zero-temperature DPRMs, the fluctuating quantity is the total energy E of the 3D pt-pt extremal trajectories. Were the simulations done at finite temperature, all connecting paths would contribute, each weighted by the appropriate Boltzmann factor; the corresponding statistical quantity would then be the restricted free energy $F = \ln Z$, analog of the height in the KPZ kinetic roughening problem. Thus, our Eulerian-Itô integrations of the $2+1$ SHE bear the same relationship to the finite-temperature DPRM as numerical studies of the KPZ equation, itself, to stochastic growth models such as Eden and ballistic deposition. The fluctuation PDFs of Fig. 1 have zero mean and unit variance, yet reveal already signature features, such as the skewness and kurtosis, of the characteristic 3D pt-pt KPZ limit distribution. Given the fine DPRM/SHE data collapse, the case for 3D KPZ class universality is clear.

We have included, too, in Fig. 1, the height fluctuation PDF of kinetic roughened *on-lattice* Eden A clusters [15], evolved to a time $t = 1000$, possessing 38 million particles in the bulk, and ≈675 000 surface sites. Thus, 15 Eden clusters yield the same 10^7 data points characteristic of our 3D pt-pt DPRM/SHE simulations; in fact, the Eden A trace in Fig. 1 follows from 200 runs, pushing us beyond the 10^{-6} probabilities managed via the DPRM/SHE. We regard these *radial* Eden A simulation results as illustrative only, however, as they rely upon a helpful, but brief intermediate temporal window, $t \approx 500$–1000, in which the model sweeps through KPZ values for the growth exponent [16] $\beta \approx 0.24^+$, skewness, and kurtosis. Our efforts here, motivated in part by recent large-scale *off-lattice* 3D Eden D results [17], are suggestive, though limited, since the small but inescapable anisotropies associated with distinct on-lattice axial and diagonal Eden A growth velocities ultimately manifest themselves globally, spoiling KPZ scaling. Even so, there are occasional, in fact, not terribly rare, instances in which a rather large, geometrically metastable, Eden A cluster can be grown, rough but unfaceted, for longer times; Fig. 1 shows (black traces) two such examples at time $t = 1750$, each containing 2.2^+ million surface particles, nestled beneath our heavily averaged DPRM/SHE PDFs and in decent agreement with them down to 10^{-3}.

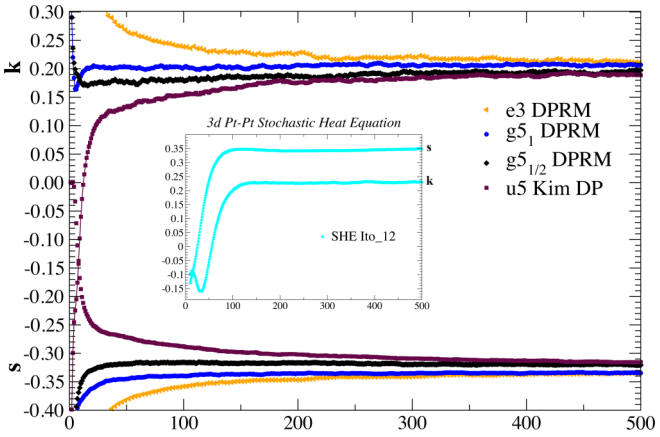

FIG. 2. (Color online) 3D *pt-pt* KPZ class: skewness s and kurtosis k.

B. Skewness and kurtosis

In Fig. 2 we show for our directed polymers the temporal evolution of the DPRM skewness $s = \langle \delta E^3 \rangle_c / \langle \delta E^2 \rangle_c^{3/2}$ and kurtosis $k = \langle \delta E^4 \rangle_c / \langle \delta E^2 \rangle_c^2$, characterizing energy fluctuations in the 3D pt-pt extremal path problem. We point out, in particular, that the kurtosis of the pt-pt $g5_1$ DPRM in this higher dimension seems nearly *devoid* of any finite-time corrections (see Fig. 2, upper trace, in blue). We have examined this interesting behavior in great detail, studying these polymers for different values of the elasticity parameter, finding that for $\gamma = 3/4$, a kurtosis $k \approx 1/5^+$ is attained within the *first half dozen steps*, remaining essentially flatlined thereafter. The 3D pt-pt DPRM skewness is only slightly less forthcoming (see Fig. 2, lower curves), where one notes that the $g5$ DP remains, again, the model of choice. A straightforward scaling analysis yields the asymptotic values for s and k recorded in Table I. Within Fig. 2 (inset), we include results from our constrained $2+1$ SHE Itô integration for $\sqrt{\epsilon} = 12$. It is apparent that the 3D pt-pt SHE is very quickly aware, as it were, of its KPZ kinship: within 100 integration time steps with $\delta t = 0.005$, the skewness has risen rapidly to $\approx$0.348, while the kurtosis plateaus at a value we measure as 0.230. For the weaker KPZ nonlinearity $\sqrt{\epsilon} = 6$, s and k climb to nearly these same values before trailing off to postplateau averages of 0.303 and 0.204, respectively. As is well known from KPZ integration work (and 3D SHE seems to be no exception), there is a delicate tradeoff involved balancing the smallness of the integration time step δt against the size of λ, numerical instabilities, etc. In any case, averaging over our four pt-pt DPRM and two SHE model simulations, we obtain $|s| = 0.328 \pm 0.014$ and $k = 0.214 \pm 0.008$, for the skewness and kurtosis, respectively, of the 3D KPZ class, confirming the *universality* of our initial $e3$ DPRM estimates [12] for these key quantities. Recent work [18] on three 3D pt-pt KPZ growth models, among them single-step (SSC) and *on-lattice* Eden D, yield values in the range $s \approx 0.32$–0.34 and $k \approx 0.20$–0.22, providing additional corroborative evidence.

C. Distilling universality

To transform the fluctuation PDFs of Fig. 1 into the limit distributions of the 3D *pt-pt* KPZ class, it is necessary to extract several nonuniversal model-dependent parameters, including (i) f_∞, the asymptotic free energy per unit length, analog of the late time growth velocity v_∞ in KPZ stochastic growth, (ii) A, the static amplitude of the fixed-time k-space height-height correlator: $\langle |h(\mathbf{k})|^2 \rangle \sim A k^{-2-2\chi}$, and, finally, (iii) the KPZ nonlinearity λ associated with each particular DPRM model. Knowledge of the last two quantities, A and λ, allows one to fix the crucial scaling combination $\theta = A^{1/\chi}\lambda$, with [12, 19] $\chi_{2+1} \approx 0.39$ the static KPZ roughness exponent [19]. With $\xi = (F - f_\infty t)/\theta^\beta$, the fundamental statistical quantity, KPZ wisdom dictates that all connected nth order cumulants $\langle \xi^n \rangle_c$ of the fundamental limit distribution $P(\xi)$ scale as $\langle \delta F^n \rangle_c / (\theta t)^{n\beta}$. Hence, looking at cumulant ratios such as s and k only gets one so far. The highest standard demands direct determination of f_∞ and θ, thus allowing explicit computation of the universal first and second moments, as well as the 3D KPZ class limit distributions proper. For the 3D pt-pt $e3$ DPRM, this entire process was initiated already [12], with an early $e3$ DPRM result published there. Fortunately, the values of θ, as well as f_∞, for $u5$ and $g5_1$ DPs were also calculated, since they were needed to pin down the $2+1$ *pt-plane* KPZ limit distribution. The requisite technology was introduced by Krug *et al.* [20] for the $1+1$ problem, but the crucial point in the present, unsolved $2+1$ case is the great utility of building the KPZ toolbox around a Krug-Meakin (KM) finite-size scaling analysis [21]. Note, in the DPRM context, the KM formula is nothing but a statistical physics variant of the Casimir effect [22]: Simulating a pt-plane $2+1$ DPRM in a rectangular box of transverse dimensions $L \times L$ results in a tiny shift Δf upwards ($\lambda < 0$ for all DPRM) of the polymer-free energy per unit length: $\Delta f = f_L - f_\infty = -\lambda A / 2L^{2-2\chi}$; see Fig. 3, inset, for results. We have collected in Table I the extracted DPRM values of f_∞ and θ, but mention specifically that for the newly considered $g5_{1/2}$, our analysis, supplemented by an examination [12] of

TABLE I. 3D KPZ universal moments, *pt-pt* DPRM geometry; equivalently, 3D Eden growth from a *point seed*.

KPZ system	$f_\infty(v_\infty)$	θ^β	$\langle \xi \rangle$	$\langle \xi^2 \rangle_c$	$\langle \xi \rangle / \langle \xi^2 \rangle_c^{1/2}$	$\lvert s \rvert$	k
$u5_1$ Kim DP	0.38390	0.71821	−2.41	0.347	4.09	0.338	0.220
$g5_1$ DPRM	−0.55336	0.98433	−2.286	0.312	4.09	0.329	0.212
$g5_{1/2}$ DPRM	−0.66593	0.83954	−2.266	0.319	4.01	0.323	0.207
$e3$ DPRM	−2.64381	4.1481	−2.24	0.304	4.06	0.335	0.212
SHE Itô-6	−0.13988	0.36136	−2.27	0.336	3.92	0.303	0.204
SHE Itô-12	−0.96884	0.21438	−2.22	0.330	3.86	0.348	0.230
Eden A*	0.21979	0.8630	−2.39	0.377	3.89	0.306	0.201

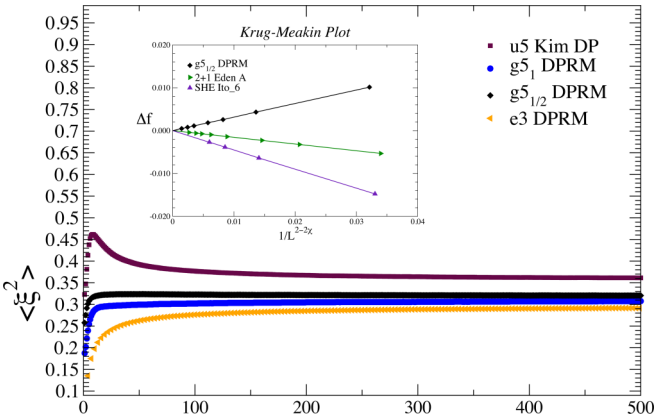

FIG. 3. (Color online) 3D *pt-pt* KPZ class: universal second moment. Inset: KM analysis: $g5_{1/2}$ DPRM, SHE Itô-6, and $2+1$ Eden A model.

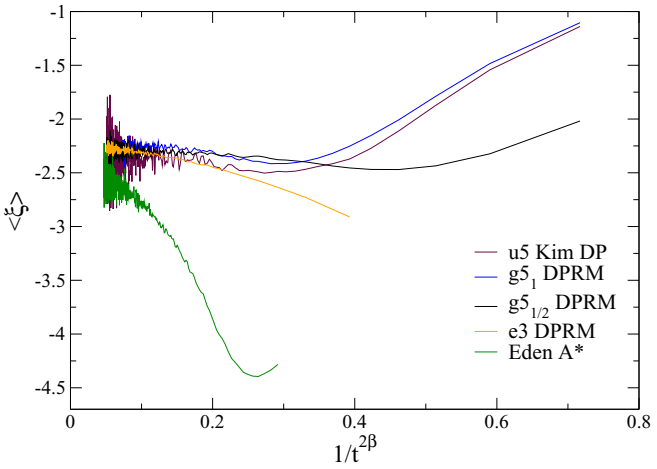

FIG. 4. (Color online) 3D *pt-pt* KPZ class: universal first moment.

the associated disorder-averaged *parabolic* DPRM free energy profile, yields $(f_\infty, A, \lambda) = (-0.665\,925, 0.849\,36, -0.7415)$, so $\theta_{g5_{1/2}} = 0.482\,51$ for this model. A similar analysis for the $2+1$ KPZ/SHE with $\sqrt{\epsilon} = 6$, produced $\theta_6 = 1.439 \times 10^{-2}$. Recalling [12] that $\theta_{e3} = 375.3$ for our $e3$ DPRM, we see that the 3D pt-pt KPZ models studied here cover *four orders of magnitude* in this key scaling parameter.

Finally, for the case of Eden, a true radial growth model, the asymptotic growth velocity is, in fact, given by the KPZ nonlinearity λ itself, providing a helpful constraint to the fit. Our results here for Eden A dictate $v_\infty = \lambda_{2+1} = 0.219\,79$ and $A_{2+1} = 1.421$, so $\theta_{EA} = 0.5411$. Noting difficulties specific to anisotropic 3D KPZ growth models [18], we revisited our on-lattice Eden system tracking specifically, over 10^6 runs, the statistics of the solitary site at the North Pole of the cluster, i.e., in the axial direction. Our findings in this regard, to which our $2+1$ KM Eden analysis is strictly applicable, with A, λ, and v_∞ appropriate to [001] and related directions, have been recorded in Table I as Eden A*. We see, in particular, that our axial Eden A* skewness and kurtosis, $s = 0.306$ and $k = 0.201$, are well in line with the DPRM/SHE results.

D. Universal variance $\langle \xi^2 \rangle$

With v_∞ and θ in hand for each of our pt-pt models (Table I), we can proceed beyond the ratios s and k, and extract the universal first and second moments, $\langle \xi \rangle$ and $\langle \xi^2 \rangle$, characteristic of the 3D KPZ limit distribution. The variance is obtained as the renormalized amplitude of the DPRM energy fluctuation: $\langle \xi^2 \rangle = \lim_{t\to\infty} \langle \delta E^2 \rangle / (\theta t)^{2\beta} \equiv a_2/\theta^{2\beta} \equiv c_2$. Here we use early notation [20], in which the model-dependent amplitude a_2, rescaled by θ^β yields the variance of the underlying limit distribution, i.e., the universal amplitude c_2 [23]. As discussed previously by Kim *et al.* [5], scaling corrections to the DPRM variance involve a simple constant term, i.e., $\langle \delta E^2 \rangle = \text{const} + c_2(\theta t)^{2\beta}$. For Eden clusters, the same insight is due to Wolf and Kertész [24]. Hence, in analyzing the data sets shown in Fig. 3, we apply a nonlinear curve fit, with $1/t^{2\beta}$ correction, extracting the *asymptotic* values for $\langle \xi^2 \rangle$, recorded in Table I. We note, in particular, that the asymptotic variance for the e3 DPRM, 0.304, represents a 4% shift upwards from the finite time $t = 500$ value, 0.291, implying a small 2% change in the distribution width. A similar finite-time effect is seen in the $u5$ DPRM, where the $t = 500$ value is 0.361; for our $g5_1$ and $g5_{1/2}$ DPs, finite-time scaling corrections are negligible; numerically, at $t = 500$, we measure 0.311 for the $g5_1$ DPRM, statistically indistinguishable from our Table I value. Averaging over DPRM/SHE models, we estimate $\langle \xi^2 \rangle^{\text{3D}}_{\text{KPZ}} = 0.325 \pm 0.016$ for the 3D pt-pt KPZ class.

E. Universal mean $\langle \xi \rangle$

Here we conclude our analysis of the 3D pt-pt KPZ class, determining the universal first moment. In this particular case, scaling corrections seem to be, as a rule, quite *strong*. We commence with the standard KPZ ansatz for the fluctuating height: $h(t) = v_\infty t + (\theta t)^\beta \xi$, from which it follows that the average instantaneous growth velocity, $\langle v(t) \rangle = \langle dh/dt \rangle$, has a finite-time correction

$$\Delta v = \langle v \rangle - v_\infty = \beta \theta^\beta \langle \xi \rangle / t^{1-\beta}$$

known, independently, by KM long ago; see, too, Ref. [23]. In Fig. 4 we investigate the asymptotics of the DPRM analog, $\langle dE/dt \rangle$, as well as the velocity shift within our axial Eden A*, where the infinite time growth velocity is known precisely. The universal first moment is given by the scaled, vanishing difference between the finite-time instantaneous growth velocity and its asymptotic value: $\langle \xi \rangle = \lim_{t\to\infty} \Delta v(t) t^{1-\beta} / \beta \theta^\beta$. It is clear that our DPs point to a universal first moment for the 3D KPZ class quite close to, but somewhat below $-2\frac{1}{4}$. In fact, we estimate, averaging over Table I DPRM model values, that $\langle \xi \rangle^{\text{3D}}_{\text{KPZ}} = -2.28 \pm 0.07$. Our axial Eden A* results, while indicating larger corrections to scaling (see Fig. 4), nonetheless suggest a value not far removed from our DPRM findings (see, again, Table I).

F. Final pass: 3D pt-pt KPZ limit distribution

In Fig. 5 we collect our DPRM/SHE results for the 3D pt-pt KPZ class limit distribution. We emphasize that our numerical characterization of the 3D pt-pt SHE appears here

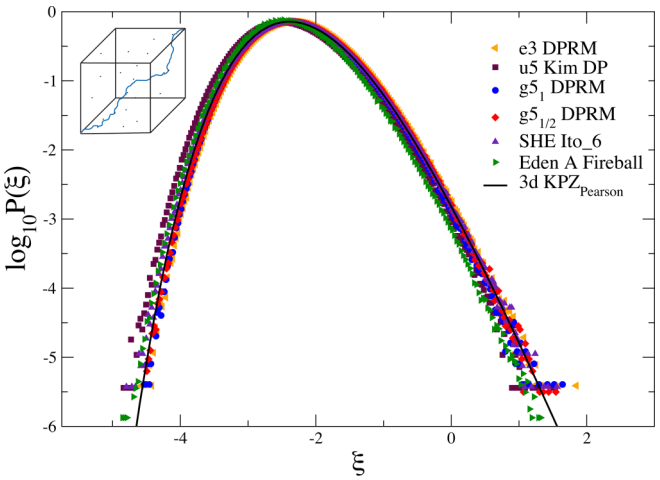

FIG. 5. (Color online) Universal limit distribution: 3D pt-pt KPZ class.

well-complemented by, and in good company with the $e3$, $g5$, and $u5$ polymer findings. We have also included, for sake of comparison, our isotropic 3D Eden A fireball results, anchored at the Eden A* mean. To give an idea of the size of the *finite-time* corrections suffered by $\langle\xi\rangle$, we note, in particular, the value previously reported [12] for the $e3$ DPRM, -1.85, is asymptotically found at -2.24, as written in Table I, a shift of $\approx$20%. In fact, this is the *smallest shift;* compare the $g5_1$ directed polymer, which at $t = 500$, is found at -1.607. Thus, to be clear, we have (grabbing them by the collar, so to speak) physically relocated in Fig. 5 each of our $t = 500$ DPRM/SHE data sets to their *independent, model-specific asymptotic positions*. We can manage this because the KM analysis, in supplying us with both v_∞ and θ, has gained us *direct access* (see Table I) to the numerical value of the asymptotic first moment $\langle\xi\rangle$ for each model. Likewise, we know the individual asymptotic variances $\langle\xi^2\rangle$ for *each model*. Ideally, all 3D KPZ class models would yield the same number, but there remain small residual differences; we doubt, in this context, whether numerical precision much beyond this is actually possible. To repeat, we have "distilled" the data sets underlying the finite-time PDFs of Fig. 1, stripping them of model-dependent baggage via the KM toolbox, rescaling the PDF width to its asymptotic value, and then translating each to its *independently determined, model-dependent* asymptotic position. All this was done in the service of four universal numbers: $\langle\xi\rangle = -2.28$, $\langle\xi^2\rangle = 0.325$, $s = 0.328$, and $k = 0.214$, which we have extracted, with great care, from the 3D pt-pt DPRM/SHE. Our goal has been to pin down this 3D KPZ limit distribution proper. Thus, we calculate and include within Fig. 5 the relevant Pearson curve [25], possessing our precisely measured values for the mean, variance, skewness, and kurtosis, discussed herein. This single curve, which captures the essence of our net DPRM/SHE analysis, provides, we believe, the most natural target against which experimental efforts on the 3D *radial* KPZ class may genuinely be compared.

A classic distribution characteristic, the mean-width ratio, was estimated previously by us for the $2 + 1$ KPZ pt-plane geometry; here we have done the same for the 3D *pt-pt* KPZ class models (see Table I). We find there the net DPRM/SHE average $\langle\xi\rangle/\langle\xi^2\rangle_c^{1/2} = 4.03 \pm 0.07$, which gives one a visceral sense of the large horizontal offset of the 3D pt-pt KPZ limit distribution [26]. The analogous quantity for the $2 + 1$ *pt-plane* KPZ class is 1.75; see below.

III. REDUX: 2 + 1 PT-PLANE KPZ CLASS

In prior work [12], devoted to the flat interface initial condition and associated $2 + 1$ KPZ class limit distribution, we made comment of a small, but persistent, dispersion among models and a slightly "stubborn approach to asymptopia of the first moment." These shifts are quite small indeed, but we return to them here, providing refined estimates. The procedure is precisely as above: we rely upon the KM finite-time correction, as well as our known model-dependent values of v_∞ and θ, quantities which are the same regardless of pt-pt, pt-line, or pt-plane geometries, all discussed in Ref. [12]. Figure 6 shows our results for various DPRM ($e3$, $u5$, $g5_1$) found in this paper, $2 + 1$ Eden A also analyzed here, the KPZ equation itself, and the classic RSOS ("restricted-solid-on-solid") model of KPZ kinetic roughening, bedrock of our previous discussion of $2 + 1$ KPZ class universality. While the numerical derivatives get increasingly noisy in the asymptotic, large-time limit, it is clear that the models converge, quite convincingly, to a common value ≈ -0.85, very near the RSOS result. Averaging over our six models, we arrive at our final estimate of the universal mean of $2 + 1$ KPZ class PDF: $\langle\xi\rangle_{\rm KPZ}^{2+1} = -0.849 \pm 0.022$; individual model values are noted in the figure legend. With variances previously reported [12], and our newly acquired $2 + 1$ Eden A value, $\langle\xi^2\rangle_c = 0.252$, we find the $2 + 1$ *pt-plane* KPZ PDF mean-width ratio: $\langle\xi\rangle/\langle\xi^2\rangle_c^{1/2} = 1.75 \pm 0.03$. We note here, too, that our exhaustive and complementary $2 + 1$ pt-plane SHE integrations for $\sqrt{\epsilon} = 6, 12$ gave values 1.70(3), 1.67(5), respectively, for this classic ratio. Also, for $\sqrt{\epsilon} = 10$, we find a limit distribution with an asymptotic skewness $s = 0.431$ and kurtosis $k = 0.362$, in fine agreement with our past $2 + 1$ KPZ results [12] for that geometry. In addition, tipping our hat to Beccaria and Curci [14], we have managed a quite solid $2 + 1$ SHE estimate for the KPZ exponent $\beta = 0.244(2)$ in

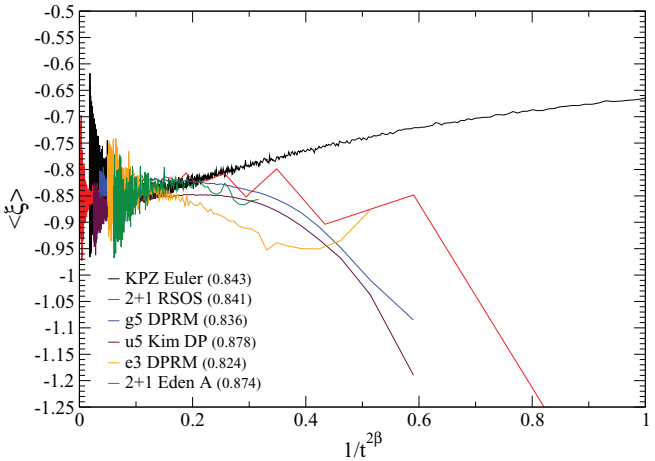

FIG. 6. (Color online) Universal first moment, $2 + 1$ KPZ class: DPRM pt-plane geometry; KPZ stochastic growth with flat interface IC.

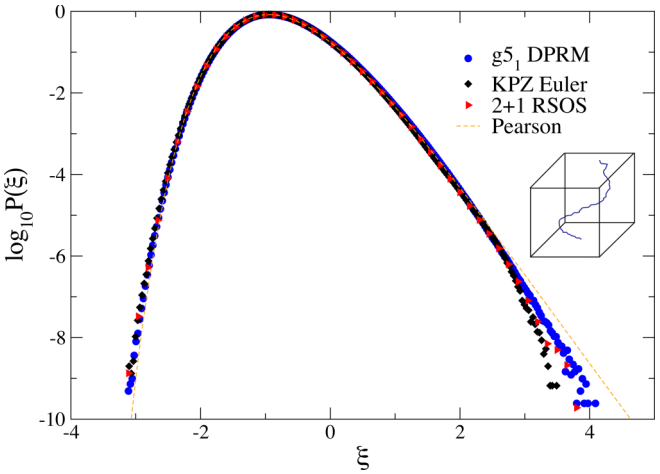

FIG. 7. (Color online) Limit distribution: $2+1$ *pt-plane* KPZ class.

this dimension. Our numerical work here on the *linear* $2+1$ SHE with multiplicative noise complements our earlier [12] straight-up Euler integration of the *nonlinear* KPZ equation with additive noise. Far from identical twins, these two siblings have rather distinct personalities in regard to numerics and certainly in the continuum, a fact much emphasized by the mathematics community [2], where the formal analysis has been based firmly on the SHE, rather than the KPZ equation itself, i.e., an ultraviolet regularization of KPZ via Hopf-Cole transformation to the SHE [13]. In Fig. 7 we record our most recent $g5_1$ DPRM and $2+1$ RSOS simulation results, with averaging now done over $nr = 1416$ and 348 runs, respectively, in a system of transverse size $L = 10^4$; we include, as well, our original KPZ Euler integration [12], involving 456 runs. The $2+1$ KPZ Pearson curve within Fig. 7 has mean $\langle\xi\rangle = -0.849$, variance $\langle\xi^2\rangle = 0.235$, skewness $s = 0.424$, and kurtosis $k = 0.346$, representing an average over all our $2+1$ *pt-plane* KPZ class models.

Finally, we mention that our specific $2+1$ RSOS result, $\langle\xi\rangle/\langle\xi^2\rangle_c^{1/2} = 1.742$, has been seen independently [18], who find $(0.324)^{-1/2} = 1.757$, and similar ratios, 1.793 and 1.762 respectively, for the $2+1$ KPZ class "etching" and SS [27] models they consider. In fact, we can do much better than this: from our previous KM analysis [12], we know that $\theta_{\rm RSOS} = 0.661\,44$, so from their *nonuniversal* amplitude [18] "g_1" $= -0.773$, we find an estimate $\langle\xi\rangle = g_1/\theta^\beta = -0.854$, supporting our own. Similarly, the second moment, $\langle\xi^2\rangle = g_2/\theta^{2\beta} = 0.1936/(0.661\,44)^{2\beta} = 0.236$, as expected, of course, given our earlier reported [12] value: 0.233. Much more interesting, perhaps, these authors also examine *pt-pt* fluctuations in a 3D *curved geometry* RSOS variant. In this case, from their nonuniversal amplitude $g_1 = -2.116$, and our $\theta_{\rm RSOS}$, we have $\langle\xi\rangle = -2.337$, a number again inaccessible to them, but in fine agreement with our precise estimate above for the 3D *pt-pt* KPZ universal first moment. Likewise, their nonuniversal RSOSC $a_2 = 0.272$, with an assist from us, translates into an RSOSC estimate $\langle\xi^2\rangle = 0.332$, in accord with our comprehensive DPRM/SHE results for the 3D pt-pt KPZ variance. As stated before, the KM analysis is applicable to all geometries; one does, however, need to examine fluctuations in the appropriate crystallographic direction.

IV. UNIVERSAL ASPECTS: 2 + 1 KPZ STATIONARY-STATE

As emphasized by Prähofer and Spohn [28] in their seminal work on $1+1$ KPZ class PNG ("polynuclear growth") model, the most fundamental distribution, potentially, is that characterizing kinetic roughening in the *stationary-state,* i.e., at later times, when the system has well-developed universal correlations dictated by the KPZ equation itself, having completely lost memory of the initial conditions. Nevertheless, because of inherent difficulties, this last case has proved the most challenging analytically. Recently, however, Imamura and Sasamoto [29] have successfully extracted the full time evolution of the $1+1$ KPZ stationary-state (SS) height fluctuation PDF to its limiting form, known from the work of Prähofer and Spohn to be the so-called Baik-Rains (BR) distribution [30] which, via the Painlevé II differential equation, possesses zero mean (by construction), variance 1.150 39, and skewness 0.359 41. In fact, the last two numbers had been carefully determined quite early in the KPZ saga (indeed, some eight years prior to the "discovery" of the BR PDF) by Krug [20], Hwa and Frey [31], and others [32,33], who had studied dynamic correlations in the $1+1$ KPZ stationary state [34]. This limit distribution is of great importance because it represents the most natural contact point of the KPZ problem and universality class to field-theoretic, mode-coupling, and associated methods. This was stressed by Hwa and Frey [31], who pointed out the crucial role played by the KPZ stationary-state distribution; these authors, however, focused their immediate attention on the dynamic height-height correlation function:

$$C(r,\Delta t) \equiv \langle [h(r_o + r, t_o + \Delta t) - h(r_o, t_o)]^2 \rangle_{t_o \to \infty},$$

where the angle brackets indicate a statistical average over the system values of r_o, the stationary state is understood via the large t_o limit, and the KPZ exponents are equally well fixed via the complementary asymptotics of the correlator: $C(r = 0,\Delta t) \sim \Delta t^{2\beta}$ and $C(r,\Delta t = 0) \sim r^{2\chi}$. Hwa and Frey argued that this truncated two-point function could be calculated exactly by a self-consistent mode-coupling analysis, at least in $1+1$, where there exists a helpful fluctuation-dissipation theorem as well as Galilean invariance, that conspire to fix $\beta = \frac{1}{3}$ and $\chi = \frac{1}{2}$. Indeed, the exact form of this scaling function was elucidated later in a second, more detailed analysis of the $1+1$ PNG model by Prähofer and Spohn [35]. Even so, it was this early work of Hwa and Frey that set the stage for a long-lived mode-coupling and field-theoretic assault [36] upon the higher-dimensional KPZ problem that continues, in various forms [37–40], unabated to the present day. We note, in particular, current efforts involving the nonperturbative renormalization group, both in its general handling [40] of the Kardar-Parisi-Zhang equation and, subsequently, with a concentrated focus upon the dimension dependence of the stationary-state scaling functions and attendant amplitude ratios [41].

A. A key observation

On the numerical side, Takeuchi [42] has revisited the $1+1$ KPZ class PNG model, returning our attention to the statistics of the *autocorrelation* function, i.e., the height

change, $\Delta h(x,\Delta t,t_o) \equiv h(x,t_o+\Delta t) - h(x,t_o)$, which gets shifted, rescaled, and relabeled by us here as

$$\xi_o = (\Delta h - v_\infty \Delta t)/(\theta \Delta t)^\beta$$

with $v_\infty = \langle dh/dt \rangle$ the asymptotic KPZ growth velocity and θ the model-dependent parameters discussed previously. Takeuchi's intriguing analysis reveals that for t_o large, one obtains the Baik-Rains and Tracy-Widom distributions in the limits $\Delta t/t_o \ll 1$ and $\Delta t/t_o \gg 1$, respectively, there being an interesting universal evolution from one limit distribution to the other as a function of the dimensionless ratio $\tau \equiv \Delta t/t_o$. One of the surprising and very useful lessons learned from Takeuchi's work is that the $1+1$ SS KPZ BR limit distribution emerges rather freely as the ratio $\Delta t/t_o$ drops below $\approx 10^{-2}$ or so; i.e., the ratio need not be vanishing small. An additional revelation of Takeuchi's $1+1$ PNG analysis, however, is the observation that a quite decent snapshot of the Baik-Rains limit distribution can be had already at $t_o = 4000$ in a system size $L = 1000$. This state of affairs seems a bit mysterious at first, since traditional KPZ lore suggests that the stationary state is not accessed till times $t_o \gg L^z$. With the dynamic KPZ exponent $z = \chi/\beta = 3/2$ given exactly in $1+1$ dimensions, it is clear that Takeuchi's *bulk* system (with $L = 1000$) is certainly *not* dynamically within the *steady-state*. One might ask, then, where his PNG system sits, so to speak, in its kinetic roughening evolution. To address this question, we recall that a key ratio in this context is the dimensionless quantity, $\xi_\parallel/L$, with $\xi_\parallel \approx (\lambda\sqrt{A}t)^{1/z}$, the parallel correlation length [20]. Additional helpful information can be had via the exact $1+1$ KPZ mode-coupling calculation of Frey *et al.* [43], which suggests that for $\lambda\sqrt{A}t/L^{3/2} \approx 0.1$, the saturation width of a generic, kinetically roughened KPZ interface has reached $\approx$90% of its asymptotic value, normalized to unity in their analysis. For Takeuchi's $1+1$ PNG model, the nonuniversal parameters are $A = 2$ and $\lambda = 2/A^2 = 1/2$, so $\lambda\sqrt{A} = 1/\sqrt{2} \approx 0.707$, the key combination $1/\lambda\sqrt{A}$ setting the *model-dependent* time scale for growth of the parallel correlation length $\xi_\parallel$. Hence, in a $1+1$ PNG simulation with $t_o = 4000$ and $L = 1000$, one has $\xi_\parallel(t_o)/L \approx 1/5$, and an interfacial width that is, roughly, 90% saturated: in other words, a bulk system that is not in the *steady-state*, but nonetheless, with well-developed nonlinear KPZ fluctuations. In fact, increasing L by a factor of five puts you further from the *steady-state*, but without much penalty, since the Frey *et al.* plot indicates 50% saturation. The essential point is to select an amply large t_o, but a sufficiently small ratio $\Delta t/t_o \lesssim 10^{-2}$. This guarantees that the correlations that evolve from a transient disturbance in the well-developed KPZ interface, which spread as $(\lambda\sqrt{A}\Delta t)^{2/3}$, remain amply, and forever, smaller than the bulk parallel correlation length by a factor $(t_o/\Delta t)^{2/3} \approx 25^+$. As is well known [20], at scales sufficiently less than the bulk parallel correlation length, the fluctuations *are, indeed, stationary.* Takeuchi has, empirically via his numerics, revealed that precise scale for us.

We have studied these things for the $1+1$ RSOS growth, where $A = 0.81$ and $\lambda = 0.78$ so, quite coincidently, for this model: $\lambda\sqrt{A} = 0.702$, a near neighbor of Takeuchi's PNG. Simulating the $1+1$ RSOS with $(\Delta t,t_o,L) = (40,4000,1000)$, tracking fluctuations of the autocorrelation height differences, we see, not surprisingly, a decent facsimile of the Baik-Rains distribution. Of course,

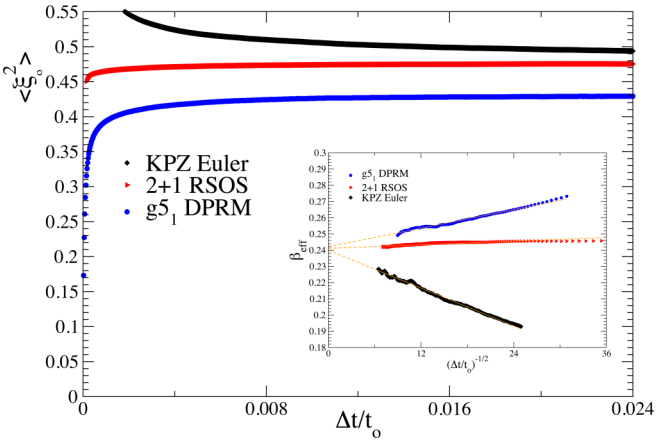

FIG. 8. (Color online) $2+1$ KPZ stationary state: universal second moment. Inset: determination of the KPZ exponent $\beta_{2+1} = 0.241(1)$, via the variance of the stationary-state fluctuations.

making a closer analysis beyond the visual impression, one finds small finite-time effects, e.g., a variance and skewness falling a bit short of their asymptotic $1+1$ KPZ Baik-Rains values [28], but to the eye, a curve that well approximates the Painlevé solution. Nevertheless, to access the KPZ exponent β via the SS height-height autocorrelation function or to press the matter further and extract more precise asymptotic values for universal moments, the present $\Delta t \approx 40$ is too small, we need a factor of 10 bigger, which demands $t_o = 40\,000$, which works. These, and other aspects of the $1+1$ KPZ class *stationary-state statistics,* we report elsewhere [44].

B. $2+1$ SS KPZ class: $\langle \xi_o^2 \rangle$ and β_{SS}

Aided by Takeuchi's insights, we examine here the higher-dimensional analog of $1+1$ KPZ Baik-Rains PDF, i.e., the universal limit distribution characterizing stationary-state fluctuations of the $2+1$ KPZ class. We gather our results for the $g5_1$ DPRM, KPZ Euler, and the RSOS models and discuss estimates for the asymptotic variance, skewness, and kurtosis of this fundamental $2+1$ *stationary-state* KPZ limit distribution. Construction of this universal PDF, requires, however, knowledge of the model-dependent parameters v_∞ and θ^β but, of course, we have those numbers in hand for the aforementioned KPZ systems (see Table I). Our analysis is very similar in spirit to that made in previous sections; e.g., we show in Fig. 8 the variance $\langle \xi_o^2 \rangle$ of the stationary-state fluctuations for this KPZ trio of models. In the case of $2+1$ RSOS and $g5_1$ DPRM, $t_o = 40\,000$, while the KPZ Euler integration (with large nonlinearity $\lambda = 20$, as in Ref. [12]) has $t_o = 10\,000$. Note, in particular, the values of $\lambda\sqrt{A}$ recorded in Table II, which reveal how much more rapidly

TABLE II. $2+1$ Stationary-state KPZ: Model results.

KPZ system	$\lambda\sqrt{A}$	β_{SS}	$\langle \xi_o^2 \rangle_c$	$\lvert s \rvert$	k
$g5_1$ DPRM	0.288	0.2421	0.445	0.240	0.18
$2+1$ RSOS	0.454	0.2411	0.480	0.256	0.18
KPZ Euler	3.03	0.2402	0.468	0.236	0.17

the parallel correlation length $\xi_\parallel$ grows for the KPZ equation itself, compared to the DPRM and RSOS models. Noting the smaller value of $\lambda\sqrt{A}$ for the $g5$ DPRM, we later ran many additional simulations for the polymer with $t_o = 80\,000$, $\Delta t = 500$, so $\tau = 6 \times 10^{-3}$. With $\Delta t/t_o$ as the plot abscissa, an appropriate comparison can be made across the models. Here one is interested, naturally, in the limit $t_o \to \infty$ first, then, secondly, $\Delta t \to \infty$. In our numerics, the ratio $\Delta t/t_o$ is kept small but manageable, per Takeuchi's observation. Thus, we collect in Table II our model-specific asymptotic estimates for $\langle \xi_o^2 \rangle$, analog of the $1+1$ KPZ Baik-Rains constant $\langle \chi_o^2 \rangle$, measured by early practitioners long ago [34]. Averaging over our three models, we report $\langle \xi_o^2 \rangle = 0.464 \pm 0.016$ as the variance of the $2+1$ *stationary-state* KPZ class limit distribution.

As an additional payoff, we note that the $2+1$ KPZ stationary-state height-height autocorrelation function provides, via the scaling of the variance, rather fine access to the fundamental scaling index β. Within the Fig. 8 inset, we show the effective exponent, defined as $\beta_{\rm eff} = \ln[w(t)/w(t/2)]/\ln 2$, for the stationary-state KPZ, RSOS, and DPRM models. As often seen for directed polymers, the DPRM exponent approaches its asymptotic value, here 0.2421, from above. Conversely, the KPZ integration generates an effective exponent that rises from below; our extracted value for KPZ Euler being 0.2402. Finally, and interestingly, the $2+1$ RSOS model, which historically has yielded somewhat larger values (≈0.245, though Ref. [12] observes 0.2422 with more exhaustive averaging) via direct measurements of the interfacial width in the *early-time* kinetic roughening phase, here shows in the stationary state a surprisingly level approach to asymptopia, intermediate between DPRM and KPZ Euler behaviors, producing 0.2411. These values are noted, as well, in Table II, where we report from our net analysis of the $2+1$ KPZ *stationary-state* autocorrelations an exponent $\beta_{2+1} = 0.241(1)$, which agrees with complementary *tour de force* simulations done in both *transient* [16] and *steady-state* [19] kinetic roughening regimes. In fact, the agreement is dead-on in the former case, at the edge in the latter. That is, by the fundamental KPZ exponent identity $\chi + \chi/\beta = 2$, this particular value yields, via the error bars, $\chi_{2+1} = 0.387$–0.390, while the independent, massive efforts of Marinari *et al*. [19] and Kelling-Odor [16], on the closely related RSOS and 2D driven dimer models, which actually produce direct measurements of the steady-state exponent, give unanimously $\chi_{2+1} = 0.393 \pm 0.003$; hence, the value $\chi \approx 0.390$ emerges as a boundary point at which the various methods might share victory. Whether, ultimately, the true 3D steady-state KPZ exponent lies slightly before or beyond this razor's edge, time will tell. From a DPRM/SHE point of a view, a slightly larger value, $\chi \approx 0.39^+$, would not be too surprising. However, the classic and very precise hypercubic stacking results of Forrest and Tang [16], as well as our own KPZ Euler integrations, which in the transient regime [12] yield $\beta = 0.2408$, and now, here, in the stationary state, 0.2402, joined by our $\beta_{\rm SS}^{\rm RSOS} = 0.2411$ above, all suggest $\chi \approx 0.39^-$. Of course, it might be wise to hedge one's bets a bit since the sacred KPZ identity is only true as an asymptotic statement. We're presently accepting wagers on the matter of 3D KPZ χ.

C. The RG connection

Interestingly, $\langle \xi_o^2 \rangle$ is, as far as we know, the only universal amplitude that has been calculated analytically for any aspect of the higher-dimensional KPZ problem. Recently Kloss *et al*. [41], hereafter referred to as KCW, have performed a field-theoretic nonperturbative renormalization group (RG) calculation of the KPZ stationary state in $1+1$, $2+1$, and $3+1$ dimensions. There they define a truncated, real-space correlator, simply related to our own: $\Delta C(\mathbf{x},t) = C(\mathbf{x},t) - C(\mathbf{0},0)$, with asymptotics for the *temporal* autocorrelation function $\Delta C(\mathbf{x}=0,t) = F_\infty t^{2\beta}$ and static *spatial* correlator $\Delta C(\mathbf{x},t=0) = F_0 x^{2\chi}$, introducing the explicit proportionality constants F_∞ and F_0, the latter, no doubt, a nice gesture to Baik and Rains [30]. From these quantities, KCW construct a universal amplitude ratio $R = |F_\infty/(F_0^{1/\chi}\lambda)^{2\beta}|$ that includes the KPZ nonlinearity λ, but is devoid of any reference to the normalization conditions that anchor the RG flows for both D and ν. Evaluated at the fixed point itself, R becomes a universal number characteristic of the $(d+1)$-dimensional KPZ class, directly related to the variance of the stationary-state fluctuations.

In regard to this quantity, the distinction between our autocorrelation function C and KCW's ΔC involves a trivial factor of two in parsing out F_∞. For $1+1$ KPZ, life is particularly simple because the Krug-Meakin shift, the k-space correlator, and the static correlation function, all share the same, identical prefactor A. Thus, in this dimension, using our own notation [23], we have $F_\infty = \frac{1}{2}\tilde{c}_2\theta^{2\beta}$, while $F_0 = A/2$. Recalling that $\theta = (\frac{1}{2})A^{1/\chi}\lambda$, we find, therefore, $R_{1+1} = 2^{2-\frac{2}{3}-1}\tilde{c}_2 = 2^{\frac{1}{3}}\tilde{c}_2$. Note the parenthetic factor of one-half in our definition of θ; this wrinkle is specific to $1+1$ KPZ and is tied to the shared legacy of KPZ, random matrix, and random sequence problems [4,28]. Given Krug's value [34] $\tilde{c}_2 = 0.712$, this implies $R_{1+1} = 0.897$, while the KCW lower-order ("NLO") and higher-order ("SO") calculations yield 0.977 and 0.945, respectively. Of course, in $1+1$, since $\tilde{c}_2 = 2^{-2/3}\langle \chi_o^2 \rangle$ the exact value $R_{1+1} = 2^{-1/3}\langle \chi_o^2 \rangle = 0.9131$ is known precisely, given in terms of the Baik-Rains constant [28,30], as discussed by Kloss *et al*. [41] and recorded in Table II of that reference. As pointed out by KCW, the accuracy of their higher-order field-theoretic RG result for the $1+1$ KPZ case is comparable to that produced by mode-coupling (MC) analyses; i.e., an error of 3%–4%, though KCW overshoot the mark, while MC methods typically yield an underestimate [31,36].

In $2+1$ and higher dimensions, there are no historical precedents to respect; here, instead, it is the Fourier integrals that must be addressed. To connect our $\langle \xi_o^2 \rangle$ to the universal amplitude R_{2+1} of KCW, we proceed in two steps. First, with a d-dimensional k-space correlator $\langle |h_k|^2 \rangle \equiv L^d k^{-(d+2\chi)}$, the prefactor of KCW's static ($t=0$) real-space truncated spatial correlation function $\Delta C(\mathbf{x},0)$, which involves the integral

$$\int_0^\infty \frac{d^d k}{(2\pi)^d} \frac{e^{i\vec{k}\cdot\vec{x}} - 1}{k^{d+2\chi}},$$

yields the anticipated spatial dependence ($\sim x^{2\chi}$), but also the numerical factor $\Gamma(-\chi)/2^{d+2\chi}\pi^{d/2}\Gamma(\chi + d/2)$. In $d=1$, where $\chi = \frac{1}{2}$, this leads to $|\Gamma(-\frac{1}{2})/4\sqrt{\pi}| = \frac{1}{2}$; i.e., the factor of two seen above in formula for F_0. In $d=2$, however, where

[12,19] $\chi_{2+1} = 0.39$, this same factor produces ≈ 0.1963, rather than one-half. The second bit of business concerns one's working definition of the parameter A. Previously [12], and in this paper as well, we have extracted A directly via the Krug-Meakin (KM) formula: $\Delta v_L = -A\lambda/2L^{2-2\chi}$. In d substrate dimensions, and with k-space correlator given as above, the KM shift is dictated by the Fourier integral

$$\int_0^{\frac{\pi}{L}} \frac{d^d k}{(2\pi)^d} k^2 \langle |h_k|^2 \rangle = \frac{S_d}{(2\pi)^d} \int_0^{\frac{\pi}{L}} dk k^{1-2\chi},$$

where $S_d = d\pi^{d/2}/\Gamma(\frac{d}{2}+1)$ for the $d+1$ KPZ problem. Performing the last integral, we retrieve the expected KM finite size dependence, $1/L^{2-2\chi}$, along with a second numerical factor, which in $d=1$ is unity, but in $d=2$ is $\pi^{1-2\chi}/2(2-\chi) \approx 0.5272$, again for $\chi_{2+1} = 0.39$ [12,19]. So, in the first instance, we have connected the k-space correlator to the static real-space correlation function prefactor F_0 and, in the second instance, to our directly measured KM FSS quantity A. Putting these two pieces together, we arrive at the direct link between the field-theoretic RG analysis of KCW and our own numerical KM-based Monte Carlo efforts: $F_0 = (0.1963)A/0.5272 = 0.3723A$. Hence, $R_{2+1} = |\frac{1}{2}\langle \xi_o^2 \rangle \theta^{2\beta}/[(0.3723A)^{1/\chi}\lambda]^{2\beta}| = 1.7062\langle \xi_o^2 \rangle$, with $2\beta/\chi = 2/z = 1.2422$, where $z = 1.61$, the $2+1$ KPZ dynamic exponent. Substituting our value for the universal $2+1$ SS KPZ variance, $\langle \xi_o^2 \rangle = 0.464(15)$, extracted as the average over $g5_1$ DPRM, KPZ Euler, and RSOS model simulations, we obtain $R_{2+1} = 0.792 \pm 0.026$, which is to be compared to the KCW NLO value, 0.940, calculated in that dimension. As suggested by KCW [41], their NLO result is likely an overestimate, a somewhat lower value (≈ 0.91, should their $1+1$ calculation be an indicator) obtained via a more thorough, so-called "SO," analysis in frequency space. Likewise, we mention that the KPZ and $2+1$ RSOS results, in themselves, with $\langle \xi_o^2 \rangle = 0.468$ and 0.480, respectively, push R to $\approx 0.81^-$, while our findings for a DPRM with *uniform*, rather that Gaussian, random site energies yield $\langle \xi_o^2 \rangle = 0.477$, with associated estimate $R_{2+1} = 0.814$. Thus, for the $2+1$ KPZ/DPRM class, we see agreement between our numerics and the nonperturbative RG calculation of KCW that, while not as impressive as the $1+1$ case, is nonetheless quite suggestive; all the more so, given KCW's comment that their method breaks down just beyond $3+1$ dimensions.

D. Stationary-state limit distribution, s and k

We have studied, too, the temporal evolution of the skewness and kurtosis of the $2+1$ RSOS, $g5_1$ DPRM, and KPZ Euler stationary-state fluctuations, recording our asymptotic estimates in Table II, and calculating average values over this KPZ trio as $s = 0.244$ and $k = 0.177$, respectively. Finally, in Fig. 9 we reveal our portrait of the $2+1$ *stationary-state* KPZ limit distribution proper, higher-dimensional analog of the $1+1$ KPZ class Baik-Rains distribution; here the three KPZ PDFs are recorded at $\Delta t/t_o = 10^{-2}$, the variances of each data set being rescaled to their *model-specific asymptotic values,* indicated in Table II. Overlaid upon the figure is the 3D SS KPZ Pearson curve, with zero mean, variance $\langle \xi_o^2 \rangle_c = 0.464$, skewness $s = \langle \xi_o^3 \rangle_c / \langle \xi_o^2 \rangle_c^{3/2} = 0.244$, and kurtosis

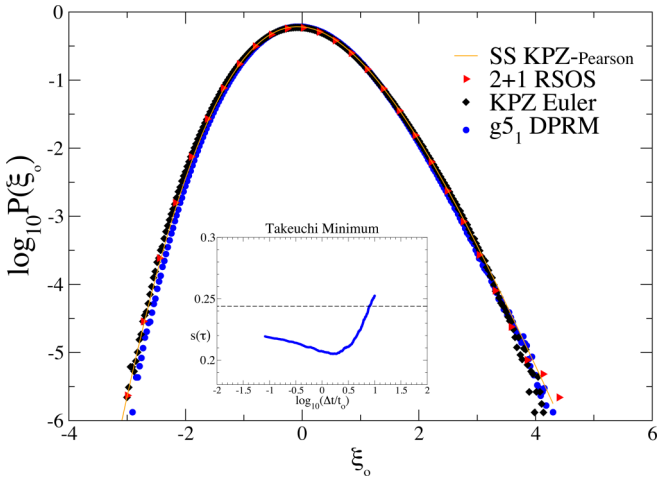

FIG. 9. (Color online) Universal limit distribution: $2+1$ KPZ *stationary-state*. Inset: Takeuchi's minimum [42], manifest within the skewness of the $2+1$ $g5$ DPRM.

$k = \langle \xi_o^4 \rangle_c / \langle \xi_o^2 \rangle_c^2 = 0.177$, reflecting our best measured values for these limit distribution characteristics.

E. Takeuchi minimum: 2 + 1 KPZ class

Within the Fig. 9 inset, we generated a semilog plot for the $2+1$ $g5_1$ DPRM skewness s versus $\tau = \Delta t/t_o$, in the heart of the crossover regime between asymptotic stationary-state ($\tau \ll 1$) and transient ($\tau \gg 1$) behaviors. The parameters here are $t_o = 500$, $50 \leqslant \Delta t \leqslant 5000$, so the dimensionless time $0.1 \leqslant \tau \leqslant 10$; our $2+1$ pt-plane simulations are done in an $L \times L$ system with $L = 7500$, averaging over 36 runs, generating a data set in excess of 2 billion points for each value of τ. Our work here is motivated by the efforts of Takeuchi [42] in the context of the PNG model, where he discovered a minimum in the $1+1$ KPZ class skewness, ≈ 0.22, well below its asymptotic Baik-Rains and Tracy-Widom GOE values, 0.3954 and 0.2935, respectively [28]. More importantly, however, the Takeuchi minimum was evident [see Ref. [42], Fig. 3(b)], in his reanalysis of the *tour de force* $1+1$ KPZ class liquid-crystal experiments, which earlier had revealed quite spectacular realizations of both the TW GUE and GOE [7] limit distributions relevant to KPZ kinetic roughening in that dimension. While the liquid-crystal work did not allow Takeuchi direct access to the Baik-Rains F_0 limit distribution [45], the skewness minimum did enable him to tease out of the data a *distinct signature* of $1+1$ KPZ class stationary-state statistics. From an experimental point of view, this is quite an impressive development, since any aspect, whatsoever, of the stationary state behavior was long thought to be inaccessible and well out of reach. Given this encouraging discovery, we have searched, ourselves, for the Takeuchi minimum in the $2+1$ KPZ class problem. Interestingly, in contrast to the lower-dimensional case, the $2+1$ stationary-state skewness is distinctly less than its transient regime counterpart; i.e., the numerical relationship reversed. In the inset of Fig. 9, we have concentrated very specifically on the sweet spot, $\tau \gtrsim 1$, of the crossover regime and find for the $2+1 g5_1$ DPRM, a Takeuchi minimum in the skewness, $s_{\rm TM} = 0.204$, at a value $\tau = 1.8$, it being quite clear that for $\tau \ll 1$, the stationary-state

value 0.244 (dashed) is approached from below, and in the opposite limit, $\tau \gg 1$, there will follow a long, steep ascent that rolls over to our value reported earlier [12], 0.424, characteristic of $2+1$ KPZ kinetic roughening with *flat initial condition*. We have performed a similar ($L = 5000$; 32 runs) investigation of the stationary-state skewness exhibited by the $2+1$ KPZ equation, itself. Our Eulerian integration there reveals a nearly identical value, $s_{TM} \approx 0.19^{+}$ and shape for the Takeuchi minimum, though the data are a bit noisier than the $g5$ DPRM (see this paper's Supplemental Materials [46]). While no doubt a coincidence, it is interesting to note the quite similar values [42,44], 0.225 and, here, ≈ 0.20, characterizing the Takeuchi minima for the $1+1$ and $2+1$ KPZ classes. One wonders whether the Takeuchi minimum might be measurable in an actual $2+1$ KPZ experiment. Recent work [47] on the kinetic roughening of 2D polymer surfaces, which have cast a preliminary eye on the height fluctuation PDFs in this higher dimension, may someday gain access, we hope, to this curious signature of the stationary-state statistics.

V. SUMMARY

We find the 3D *pt-pt, pt-plane*, and *stationary-state* KPZ classes present numerous intriguing challenges and opportunities. From an experimental point of view, attention might best be focused, initially, upon the $2+1$ pt-plane problem, i.e., KPZ kinetic roughening from a flat initial condition, since large lateral system sizes can provide ready access to the *transient regime* skewness $\bar{s} = 0.424$ and kurtosis $\bar{k} = 0.346$ [12], along with the all-important height fluctuation PDF, which highlights already (e.g., Fig. 1 in Ref. [12]) these elemental features of the underlying limit distribution. While measurement of the asymptotic growth velocity v_∞ ought to be straightforward, direct experimental extraction of the system-dependent parameter $\theta = \lambda A^{1/\chi}$ will be difficult. Of course, a quick (short-cut) determination of θ^β could be accessed from the *nonuniversal* amplitude a_2 of the variance, relying upon our established value $\langle \xi^2 \rangle^{\rm KPZ}_{2+1} = 0.235$. See Sec. II D., where we discuss, in detail, such matters; see also Refs. [20,23]. This is the manner in which Takeuchi and Sano analyzed their $1+1$ *flat* KPZ class data. In any case, with θ^β in hand, (1) an estimate could then be had for the universal first moment, compared to our $\langle \xi \rangle^{\rm KPZ}_{2+1} = -0.849$, (2) transformation made of the zero-mean, unit-variance height fluctuation PDF into the fundamental $2+1$ *pt-plane* KPZ limit distribution proper, and (3) the experimental distribution overlaid with the requisite Pearson curve. Of course, knowledge of θ is *not* necessary to find the mean-width ratio of this limit distribution since $\langle \xi \rangle / \sqrt{\langle \xi^2 \rangle_c} = a_v / \beta \sqrt{a_2}$, with a_v, the *nonuniversal* finite-time correction amplitude to v_∞ [20,23], very likely the most formidable quantity for the resourceful experimentalist to pin down, as it requires exhaustive averaging to quell the numerical derivatives. Our estimate of this characteristic quantity for the $2+1$ pt-plane KPZ class is (recall Sec. III) $\langle \xi \rangle / \sqrt{\langle \xi^2 \rangle_c} = 1.75$. Last, concentrating on the temporal correlations hidden within the dynamically evolving height fluctuations, one can [42] slice across the huge raw data sets for various values of t_o, Δt, and $\tau = \Delta t / t_o$, studying the functional dependence of skewness $s(\tau)$, per Takeuchi in the $1+1$ KPZ class liquid-crystal experiments. Recall, this business demands, in a first pass, no knowledge of model-dependent parameters, but might provide access to a precursor signature of the $2+1$ KPZ class stationary-state statistics. Accessing the higher dimensional analog (see Fig. 9) of the $1+1$ KPZ class Baik-Rains distribution will, however, require some heavy lifting or a very clever idea indeed.

All this is in marked contrast to the $1+1$ KPZ class experimental situation, where the flat and circular geometries were, more or less, on equal footing. In fact, historically, the liquid-crystal experiments [7] privileged the radial case first, since it rendered moot the issue of boundary conditions. Furthermore, the KPZ kinetic roughening equivalence $\lambda = v_\infty$, peculiar to that curved geometry, greatly facilitated the analysis, leaving only A to be fixed via the spatial correlation function. In three dimensions, this equivalence remains valid; however, because of the strong finite-time corrections inherent to the radial problem, discussed in Sec. II E and elsewhere [18], an initial experimental foray into the matter might search quite specifically for the skewness ($\approx 1/3^-$) and kurtosis ($\approx 1/5^+$), the latter a particularly salient indicator of this 3D *pt-pt* KPZ class; see Sec. II B. Excellent value, too, is had via simple height fluctuation PDFs, such as in Fig. 1. Finally, a compelling experimental realization of the 3D KPZ exponent $\beta \approx 1/4^-$ would be most welcome, recent devotion to limit distributions notwithstanding. In any case, we have, due to Fig. 5, a pretty solid portrait of the 3D pt-pt KPZ class limit distribution at our disposal.

We stress too, in closing, the benefits of cross-geometry, isotropic experiments where possible. Once the model-dependent parameter θ is known, it applies in *all* KPZ settings: pt-pt, pt-line, and pt-plane, as well as stationary-state statistics. Thus, one might determine the KPZ nonlinearity λ from the asymptotic growth velocity in a radial geometry, and the parameter A from the rectangular setup; θ is then known. Admittedly, this is a tall order. On the flip side, however, this suggests the existence of additional universal quantities that, while characteristic of 3D KPZ universality *more broadly*, are (i) like s and k, independent of θ, but (ii) cut across KPZ class boundaries, and (iii) are, potentially, of practical value to the experimentalist, since they can be immune to scaling eccentricities of individual models. A case in point that we specifically highlight is the quantity $\langle \xi^2 \rangle^{\rm 3D}_{\rm pt\text{-}pt} / \langle \xi^2 \rangle^{2+1}_{\rm pt\text{-}plane} = \lim_{t\to\infty} \langle \delta E(t)^2 \rangle^{\rm 3D}_{\rm pt\text{-}pt} / \langle \delta E(t)^2 \rangle^{2+1}_{\rm pt\text{-}plane}$, a ratio of variances, but in fact of *nonuniversal* amplitudes, whose time dependence can be readily plotted up and tracked and, crucially, avoids the numerical derivatives. For our own $u5$ and $g5_1$ DPRM models, we estimate for this quantity, 1.39 and 1.41, respectively, i.e., quite similar values, despite the fact that the Gaussian polymer is, figuratively speaking, much closer initially to the KPZ fixed point than its uniform disorder counterpart. Thus, this cross-geometry *ratio of variances*, like the mean-to-width ratio *within* an individual KPZ class (note our Table I entries for $u5$ and $g5_1$ DPRM 3D pt-pt problem) can be quite forgiving. Similarly, for $e3$ DPRM, we find 1.43, while for 3D curved and flat RSOS(C) models [18] a ratio of nonuninversal amplitudes "g_2": $0.272/0.1936 = 1.405$, corroborating our idea. Along similar lines, we have also examined the θ-independent, cross-KPZ class ratios: $\langle \xi^2 \rangle^{2+1}_{\rm SS} / \langle \xi^2 \rangle^{2+1}_{\rm pt\text{-}plane} = 1.98$, following from the stationary-state models listed in our Table II, and $\langle \xi^2 \rangle^{\rm 3D}_{\rm pt\text{-}line} / \langle \xi^2 \rangle^{2+1}_{\rm pt\text{-}plane} = 1.137$, in the latter instance, with surprisingly nearly identical values for the $e3$ and $g5_1$ DPRM.

Of course, from a mathematical point of view, it is the underlying superuniversal architecture supporting such structure, ratios, and limit distributions, analogous to Painlevé II, a Fredholm determinant expression, or novel $1+1$ DPRM RG reformulation [48], that we'd like to get our hands on in this higher dimension. Interestingly, from a biological perspective, it has been recently suggested [49], via first passage percolation ideas, that the $2+1$ *flat* KPZ class limit distribution might bear relevance to spatial evolution models of cancer progression in planar habitats, i.e., a KPZ statistics of "waiting times to cancer." [50]. One wonders, naturally then, with the 3D pt-pt KPZ class limit distribution now well characterized and in hand, of a related connection to the *radial* growth of tumors [51].

ACKNOWLEDGMENTS

We are grateful to Giorgio Parisi who, following Ref. [12], gave a gentle reminder regarding scaling corrections. Many thanks, as well, to Joachim Krug for shared wisdom, and his many helpful comments concerning early versions of this manuscript.

APPENDIX: 3D PT-LINE KPZ CLASS

Beyond the canonical pt-pt and pt-plane formulations, the DPRM in three dimensions allows for an additional, very natural subclass, that associated with the *pt-line* geometry. In this instance, one is concerned with the globally optimal directed path which, emanating from the origin, is constrained to terminate along a fixed line within the plane of a later time slice. In the KPZ context, the analogous process corresponds to stochastic growth initiated from a 1D linear source, being essentially KPZ droplet growth within a groove, i.e., a trough of triangular cross section. We introduced the 3D pt-line DPRM earlier [12], where we considered solely the $e3$ directed polymer in this geometry, that is, the extremal trajectory traveling on average in the [111] direction through a random medium with unit mean, exponentially distributed energies on the lattice sites. There we discovered a distinct pdf for the pt-line geometry. We provide, here, additional model results, establishing universality of this particular limit distribution. In Table III we show for the $e3$, $g5_1$, and $g5_{1/2}$ DPRM, as well as the constrained pt-line SHE with $\lambda = 12$, our extracted estimates for the asymptotic values of the first four moments of the 3D *pt-line* KPZ class limit distribution. For the pt-pt problem, our numerical integration of the stochastic heat equation followed the fate of $Z(\mathbf{x}=\mathbf{0},t)$ subject to the delta-function initial condition (IC): $Z(\mathbf{x},t=0)=\delta(\mathbf{x})$. Of course, for the pt-line problem on hand, we have at $t=0$: $Z=1$ everywhere along, let's say, the x axis, zero otherwise. In

TABLE III. Universal quantities: 3D *pt-line* KPZ problem.

KPZ system	$\langle\xi\rangle$	$\langle\xi^2\rangle_c$	$\langle\xi\rangle/\langle\xi^2\rangle_c^{1/2}$	$\lvert s\rvert$	k
e3 DPRM	−1.45	0.245	2.93	0.383	0.282
$g5_{1/2}$ DPRM	−1.49	0.254	2.96	0.397	0.302
$g5_1$ DPRM	−1.497	0.251	2.99	0.398	0.306
SHE Itô-12	−1.44	0.245	2.91	0.407	0.346

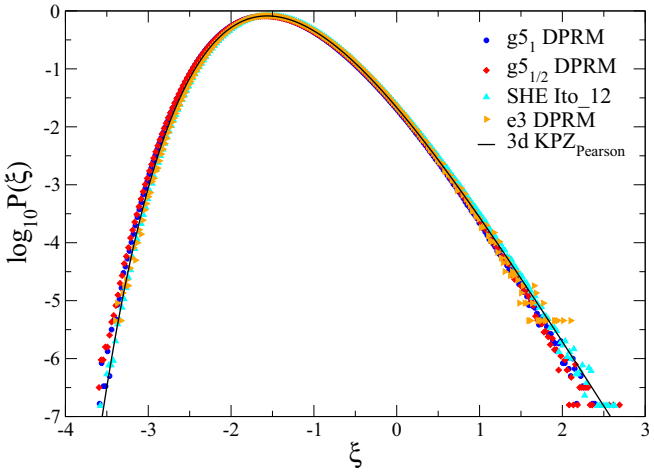

FIG. 10. (Color online) Limit distribution: 3D *pt-line* KPZ class.

$1+1$ dimensions, recall, it is the sharp wedge IC for $F=\ln Z$, that appears in the exact solution of the KPZ equation itself. The constrained $2+1$ pt-line SHE merely extends this wedge in a second dimension, while the 3D pt-pt problem rotates it about the z axis generating a conical IC. Again, we follow the spatiotemporal evolution of $Z(\mathbf{0},t)$; i.e., the probabilistic weight of an endpoint above the origin. It should be stressed that for the complementary zero-temperature Gaussian $g5_{1/2\&1}$ DPRM, which we consider on a cubic lattice and proceeding in the [001] direction, we gain, thanks to the formulation of Kim *et al.* [5], a factor of L over our $e3$ simulations, where each run generates only a single pt-line extremal path. This is evident in Fig. 10, where we consider the universal limit distribution governing the statistics of the shifted, rescaled 3D pt-line DPRM (free) energy fluctuation:

$$\xi' = \frac{F - f_\infty t}{(\theta t)^\beta}$$

with f_∞, as before, the polymer's asymptotic free energy per unit length and θ^β, the key model-dependent scale factor; see Table I in the main body of the paper for values. We emphasize, again in this context, that the parameters f_∞, A, λ, and therefore $\theta = A^{1/\chi}\lambda$ cut across different geometric classes (pt-pt, pt-line, and pt-plane); i.e., once determined by Krug-Meakin in the pt-plane setup, the same f_∞ and θ^β applies to them all. In any case, one notes immediately in Fig. 10 the data collapse for the four systems, with probabilities extending down to 10^{-7}, two orders of magnitude or so better than our efforts in the most challenging pt-pt geometry, but still shy of the 10^{-9} or so achieved for the pt-plane problem, which contribute, per run, a very welcome L^2 data points to the ensemble average. For the pt-line case discussed here, we made 2500 runs each for the Gaussian polymers, $g5_{1/2}$ and $g5_1$, 6500 runs for the $\lambda = 12$ SHE, and finally, 10^7 realizations of the $e3$ DPRM. Our analysis for the $g5_{1/2\&1}$ and SHE12 were done in an $L \times L \times t$ rectangular box with $L = 10^4$, $t = 500$, and periodic BC.

In regard to our individual model results for the 3D pt-line KPZ class (see Table III), we observe that the asymptotic values recorded there for the mean, variance, skewness, and

kurtosis show quite good agreement. Averaging over models, we obtain $\langle \xi \rangle = -1.469 \pm 0.025$, and $\langle \xi^2 \rangle_c = 0.2485$, with an associated mean-to-width ratio $\langle \xi \rangle / \sqrt{\langle \xi^2 \rangle_c} = 2.94$, intermediate to the pt-pt and pt-plane values, 4.03 and 1.75, respectively, for this characteristic quantity. In addition, we note for this pt-line geometry, an average asymptotic skewness, $|s| = 0.396$, and kurtosis, $k = 0.309$, not far from our initial finite-time $t = 500$ values [12], 0.402 and 0.305, respectively, first reported for the $e3$ DPRM. We mention, too, preliminary results, not shown, for the $u5$ DPRM in three dimensions, which yield, consistently, $|s| = 0.408$ and $k = 0.322$, for this 3D pt-line directed polymer subject to uniform random noise. Finally, we have begun examining 3D RSOS KPZ kinetic roughening in a groove, which indicates $|s| = 0.381$, though the kurtosis appears a bit low. As is customary, we have fitted our DPRM/SHE data of Fig. 10 with the Pearson curve possessing the requisite, carefully determined values for the first four moments of the 3D *pt-line* KPZ universal limit distribution.

[1] D. A. Huse and C. L. Henley, Phys. Rev. Lett. **54**, 2708 (1985); for an early attempt at the 3D extremal path problem in random media, see M. Kardar and Y.-C. Zhang, *ibid.* **58**, 2087 (1987).

[2] T. Sasamoto and H. Spohn, Phys. Rev. Lett. **104**, 230602 (2010); G. Amir, I. Corwin, and J. Quastel, Commun. Pure Appl. Math. **64**, 466 (2011); P. Calabrese, P. Le Doussal, and A. Rosso, Europhys. Lett. **90**, 20002 (2010); V. Dotsenko, *ibid.* **90**, 20003 (2010).

[3] C. A. Tracy and H. Widom, Commun. Math. Phys. **159**, 151 (1994); **177**, 727 (1996); **207**, 665 (1999); also, J. Baik, P. Deift, and K. Johansson, J. Am. Math. Soc. **12**, 1119 (1999).

[4] T. Kriecherbauer and J. Krug, J. Phys. A. **43**, 403001 (2010); I. Corwin, Random Matrices: Theor. Appl. **1**, 1130001 (2012); The link between the $1+1$ *curved* KPZ class and the Gaussian unitary ensemble (GUE) of random matrix theory was made by K. Johansson, Commun. Math. Phys. **209**, 437 (2000); see also M. Prähofer and H. Spohn [28], who elucidated the connection of $1+1$ *flat* KPZ growth to Gaussian, orthogonal (GOE) matrices, as well as the relevance of the Baik-Rains F_0 distribution [30] to $1+1$ KPZ *stationary-state* statistics.

[5] J. M. Kim, M. A. Moore, and A. J. Bray, Phys. Rev. A **44**, 2345 (1991); T. Halpin-Healy, *ibid.* **44**, R3415 (1991).

[6] L. Miettinen, M. Myllys, J. Merikoski, and J. Timonen, Eur. Phys. J. B **46**, 55 (2005).

[7] K. A. Takeuchi and M. Sano, Phys. Rev. Lett. **104**, 230601 (2010); for $1+1$ *flat* KPZ class experiments, see K. Takeuchi, M. Sano, T. Sasamoto, and H. Spohn, Sci. Rep. **1**, 34 (2011); K. A. Takeuchi and M. Sano, J. Stat. Phys. **147**, 853 (2012); K. A. Takeuchi, arXiv:1310.0220.

[8] T. Halpin-Healy and Y.-C. Zhang, Phys. Rep. **254**, 215 (1995); J. Krug, Adv. Phys. **46**, 139 (1997).

[9] M. Gorissen, A. Lazarescu, K. Mallick, and C. Vanderzande, Phys. Rev. Lett. **109**, 170601 (2012).

[10] A. Parmeggiani, Physics **5**, 118 (2012).

[11] M. Kardar, G. Parisi, and Y.-C. Zhang, Phys. Rev. Lett. **56**, 889 (1986); see too H. van Beijeren, R. Kutner, and H. Spohn, *ibid.* **54**, 2026 (1985); D. A. Huse, C. L. Henley, and D. S. Fisher, *ibid.* **55**, 2924 (1985) for crucial parallel work.

[12] T. Halpin-Healy, Phys. Rev. Lett. **109**, 170602 (2012).

[13] J. Quastel, Introduction to KPZ (unpublished).

[14] M. Beccaria and G. Curci, Phys. Rev. E **50**, 4560 (1994); these authors estimate the early-time KPZ roughness exponent $\beta_{2+1} = 0.240(1)$, corroborating earlier findings of Forrest and Tang [16].

[15] S. G. Alves, T. J. Oliveira, and S. C. Ferreira, Europhys. Lett. **96**, 48003 (2011); also, L. R. Paiva and S. C. Ferreira, J. Phys. A **40**, F43 (2007).

[16] B. M. Forrest and L.-H. Tang, Phys. Rev. Lett. **64**, 1405 (1990); $\beta_{2+1} = 0.240(1)$; see also J. Kelling and G. Ódor, Phys. Rev. E **84**, 061150 (2011), who report 0.2415(15).

[17] S. G. Alves and S. C. Ferreira, J. Stat. Mech. (2012) P10011; in particular, their Fig. 4, which shows an increasing skewness, $s \approx 0.25$ at $t = 700$, but a kurtosis that is, stubbornly, still *negative* at this time.

[18] T. J. Oliveira, S. G. Alves, and S. C. Ferreira, Phys. Rev. E **87**, 040102 (2013); these authors consider cumulant ratios only, with no direct access to $\langle \xi \rangle$ or $\langle \xi^2 \rangle$.

[19] E. Marinari, A. Pagnani, and G. Parisi, J. Phys. A **33**, 8181 (2000); $\chi_{2+1} = 0.393(3)$; note that, via the fundamental KPZ identity, $\chi + z = 2$, with $z = \frac{\chi}{\beta}$, implies $\beta = 0.245(2)$. Here one works with small systems sizes L, strictly in the steady state, $t \gg L^z$, studying the saturation width scaling. The associated *steady-state* height fluctuation PDF was also investigated by Y. Shim and D. P. Landau, Phys. Rev. E **64**, 036110 (2001); see too F. D. A. Aarão Reis, *ibid.* **69**, 021610 (2004); Kelling and Ódor [16], Fig. 6, represents an impressive culmination of these earlier efforts, focusing on the $2+1$ KPZ steady-state *width* fluctuation PDF. Recall, for the $1+1$ KPZ class, the steady-state height PDF is Gaussian, quite distinct from the Baik-Rains limit distribution controlling *stationary-state* fluctuations in that dimension.

[20] J. Krug, P. Meakin, and T. Halpin-Healy, Phys. Rev. A **45**, 638 (1992).

[21] J. Krug and P. Meakin, J. Phys. A **23**, L987 (1990).

[22] M. E. Fisher, J. Stat. Phys. **34**, 667 (1984); J. Krug and L.-H. Tang, Phys. Rev. E **50**, 104 (1994).

[23] We note, in this context, that for the $1+1$ KPZ universality class, KMHH [20] had obtained $c_2 = 0.404$, which yields the variance $\langle \chi_1^2 \rangle_c = 2^{2/3} c_2 = 0.641$, anticipating the TW-GOE value, 0.638 05, nailed down later by Tracy and Widom via Painlevé II [3]. Close to the mark, as well, KMHH had for the first moment: $\langle \chi_1 \rangle = 3 \times 2^{1/3} c_v = -0.7295$, with $c_v = -0.193$, the universal *finite-time* correction to the asymptotic KPZ growth velocity $\langle dh/dt \rangle$.

[24] D. E. Wolf and J. Kertesz, Europhys. Lett. **4**, 651 (1987).

[25] Pearson Type IV, trigonometrical case; easily calculable from our four 3D KPZ moments, but readily supplied by the author. Likewise, a zero mean, unit variance version appropriate to Fig. 1. Of historic value, we note the classic work K. Pearson, Phil. Trans. R. Soc. Lond. A **186**, 343 (1895); See also S. T. Bramwell *et al.*, Phys. Rev. E **63**, 041106 (2001); who, in the not-too-distant context of nonequilibrium dynamics of classical XY magnets, provide an ample discussion of various asymmetric, skewed PDF fitting functions (Pearson, Gumbel, Log Normal,

etc.), all of which do quite well down to probabilities 10^{-5} or so but, of course, ultimately possess the wrong tails for the problem at hand. In separate work, we discuss the various virtues and vices of these fitting functions for the KPZ problem.

[26] To this one might compare the value $\approx(0.061)^{-1/2}$ obtained in Ref. [18] for RSOSC and Takeuchi Eden D models.

[27] Identical to 2D driven dimers, studied previously in Ref. [12].

[28] M. Prähofer and H. Spohn, Phys. Rev. Lett. **84**, 4882 (2000); For the $1+1$ *stationary-state* KPZ class limit distribution, these authors record the Baik-Rain values for the universal quantities: $\langle\chi_o\rangle = 0$, $\langle\chi_o^2\rangle = 1.150\,39$, skewness $s = 0.359\,41$, and kurtosis $k = 0.289\,16$.

[29] T. Imamura and T. Sasamoto, Phys. Rev. Lett. **108**, 190603 (2012); J. Stat. Phys. **150**, 908 (2013).

[30] J. Baik and E. M. Rains, J. Stat. Phys. **100**, 523 (2000).

[31] T. Hwa and E. Frey, Phys. Rev. E **44**, R7873 (1991).

[32] L.-H. Tang, J. Stat. Phys. **67**, 819 (1992).

[33] J. Amar and F. Family, Phys. Rev. A **45**, 5378 (1992).

[34] Sec. VI, KMHH [20], notes at $t = 10^3$, $\tilde{c}_2 = 0.712$, which yields $\langle\chi_o^2\rangle = 2^{2/3}\tilde{c}_2 = 1.13^+$, while for the $1+1$ *stationary-state* KPZ class skewness, Krug obtained $s = 0.33$, both numbers in fine agreement with those unearthed much later by Prähofer and Spohn [28]. Following Krug, independent estimates of $\tilde{c}_2$ were made, too, by Hwa and Frey [31]: 0.69, Tang [32]: 0.725 ± 0.005, as well as Amar and Family [33]: 0.71. Interestingly, Tang's value, implying $\langle\chi_o^2\rangle = 1.150\,87$, relies upon a *finite-time* scaling analysis and $t^{-2\beta}$ correction; as such, it is a true asymptotic estimate, stunningly prescient in its accurate assessment of the Baik-Rains constant [28]. The roots of this intriguing number can be traced back to the 1985 BKS work on driven diffusive systems [11]. A recent variation on the theme is due to C. Mendl and H. Spohn, arXiv:1305.1209.

[35] M. Prähofer and H. Spohn, J. Stat. Phys. **115**, 255 (2004).

[36] J.-P. Bouchaud and M. E. Cates, Phys. Rev. E **47**, R1455 (1993); Y. Tu, Phys. Rev. Lett. **73**, 3109 (1994); M. A. Moore, T. Blum, J. P. Doherty, M. Marsili, J.-P. Bouchaud, and P. Claudin, *ibid.* **74**, 4257 (1995); F. Colaiori and M. A. Moore, *ibid.* **86**, 3946 (2001).

[37] M. Lässig and H. Kinzelbach, Phys. Rev. Lett. **78**, 903 (1997); M. Lässig, *ibid.* **80**, 2366 (1998); C.-S. Chin and M. den Nijs, Phys. Rev. E **59**, 2633 (1999).

[38] H. C. Fogedby, Phys. Rev. Lett. **94**, 195702 (2005); Phys. Rev. E **73**, 031104 (2006).

[39] L. Canet and M. A. Moore, Phys. Rev. Lett. **98**, 200602 (2007)

[40] L. Canet, H. Chaté, B. Delamotte, and N. Wschebor, Phys. Rev. Lett. **104**, 150601 (2010); Phys. Rev. E **84**, 061128 (2011); an early functional RG treatment of the many-dimensional DPRM: T. Halpin-Healy, Phys. Rev. Lett. **62**, 442 (1989).

[41] T. Kloss, L. Canet, and N. Wschebor, Phys. Rev. E **86**, 051124 (2012); see esp. Sec. IVE.

[42] K. A. Takeuchi, Phys. Rev. Lett. **110**, 210604 (2013).

[43] E. Frey, U. C. Täuber, and T. Hwa, Phys. Rev. E **53**, 4424 (1996); see, in particular, their Fig. 3, and associated text.

[44] T. Halpin-Healy and Y. Lin, manuscript; these authors, examining RSOS, SHE-Itô, and Gaussian DPRM models, locate the Takeuchi minimum of the $1+1$ KPZ class skewness at $s_{\rm TM} = 0.225 \pm 0.005$, for $\tau = \frac{\Delta t}{t_o} = 4.5 \pm 0.4$.

[45] In the $1+1$ KPZ class liquid crystal experiments, the largest t_o was 1 minute, but it has been estimated [42] that substantially longer runs, of order $\approx$1000s, are necessary to render a convincing portrait of the BR distribution; alternatively, a deft realization of SS KPZ initial condition.

[46] See Supplemental Material at http://link.aps.org/supplemental/10.1103/PhysRevE.88.042118 for the Takeuchi minimum: $2+1$ KPZ equation, itself.

[47] T. A. de Assis *et al.*, J. Phys.: Condens. Matter **25**, 285106 (2013).

[48] M. Hairer, Ann. Math. **178**, 559 (2013).

[49] J. Otwinowski and J. Krug, arXiv:1302.4326.

[50] E. A. Martens, R. Kostadinov, C. C. Maley, and O. Hallatschek, New J. Phys. **13**, 115014 (2011).

[51] See, e.g., for the 2D radial KPZ class and edge roughening of cell colonies M. A. C. Huergo, M. A. Pasquale, P. H. González, A. E. Bolzán, and A. J. Arvia, Phys. Rev. E **85**, 011918 (2012); **84**, 021917 (2011); see also O. Hallatschek, P. Hersen, S. Ramanathan, and D. R. Nelson, Proc. Natl. Acad. Sci. USA **104**, 19926 (2007); M. Block, E. Schöll, and D. Drasdo, Phys. Rev. Lett. **99**, 248101 (2007); a preliminary foray into the 3D radial growth problem is M. Radszuweit, M. Block, J. G. Hengstler, E. Schöll, and D. Drasdo, Phys. Rev. E **79**, 051907 (2009).